TECHNICAL PAPER

Analysis and modelling of thrust force in drilling of basalt and carbon fibre-reinforced polymer (BFRP and CFRP) composites

Gergely Magyar[1] · Norbert Geier[1]

Abstract

Currently, the use of sustainable products and technologies is growing; consequently, mineral-origin basalt fibre-reinforced polymer (BFRP) composites are becoming more popular in industries. Although BFRP parts require mechanical drilling operations for manufacturing holes for assembly, many challenges make the drilling process difficult. Considering that the cutting force is one of the main parameters characterising the drilling process, this study aims to analyse the influence of feed (mm/rev) and cutting speed (m/min) on the thrust force and model the thrust force in the drilling of BFRP composites through response surface methodology (RSM) and advanced statistical modelling methods. In order to determine main and interaction effects and to calculate the regression coefficients and model parameters, mechanical drilling experiments were performed, and the thrust force was recorded. The raw force data were processed using fast Fourier transformation-based low-pass filtering, and then the calculated thrust force parameters were evaluated relative to various feeds and cutting speeds. In addition, results were compared with those of carbon fibre-reinforced polymer composites. The results of the validation experiments show that both RSM and advanced statistical models accurately predict the thrust force in BFRPs of 96.74% and 95.01%, respectively. However, the advanced statistical model can describe not only the maximum values of the force but also its characteristics at a coefficient of determination of 0.68.

Keywords BFRP · CFRP · Drilling · Cutting force · RSM

1 Introduction

Fibre-reinforced polymer (FRP) composites have been used for many years in high-end industries mainly due to their excellent specific mechanical properties [1–3]. Glass and carbon fibres are the most used reinforcing materials in the high-end industries [4, 5]. However, their manufacturing is costly, and the life cycle of products made from carbon and glass fibres is relatively short. Their recycling and/or reusing is difficult or often not solvable [6–8]. Therefore, researchers developed novel fibrous composites using organic and inorganic reinforcing fibres. Hence, basalt fibres having mineral

origin become the focus of attention [9]. Basalt fibres provide a suitable insulation property, high elasticity modulus, excellent heat and acoustic resistance, and are outstanding vibration isolators [10]. Czigány et al. [9] highlighted that application of basalt as reinforcing fibres in polymer composites is highly recommended and will be spread in the forthcoming years. Although material scientists revealed numerous advantageous properties of basalt fibre-reinforced polymer (BFRP) composites [11–14], their spread is inhibited due to the lack of knowledge on their machinability.

Amuthakkannan et al. [15] were among the first authors to scientifically investigate the drilling of BFRP composites. In their research, the authors focused on optimising the technological parameters of drilling BFRP composite to minimise delamination (separation between plies, which may cause the destruction of structural parts resulting in decreased resultant strength). Their results showed that optimal results could be reached by selecting the lowest feed rate tested. Several studies [16–19] have shown that the selection of the lowest feed rate for drilling fibre-reinforced polymer composites results in the lowest thrust force (cutting force

---

✉ Norbert Geier
geier.norbert@gpk.bme.hu

1 Department of Manufacturing Science and Engineering, Faculty of Mechanical Engineering, Budapest University of Technology and Economics, Műegyetem Rkp. 3, Budapest 1111, Hungary

component parallel to the axis of the cutting tool), which also has a positive effect on the drilling-induced delamination. However, this research did not make direct empirical connections between thrust force and delamination during drilling.

Navarro-Mas et al. [20] first studied the phenomenon of tool wear through BFRP composite edge trimming experiments. The authors performed their edge trimming experiments using an uncoated cutting insert tool. They have found that the cutting speed has the most significant effect on tool wear. The tool wear often affects the delamination, which they tested in further experiments. However, no information was published about the actual cutting force while drilling BFRP composite in this or in their upcoming studies. It has been proven that the cutting force significantly affects the occurring delamination.

Navarro-Mas et al. [21, 22] found that the drilling-induced delamination has a lower probability of formation at lower feed rates at edge trimming BFRP composites. Presumably, this is due to the fact that the smaller feed rate reduces the chip cross section, resulting in a lower cutting force, although a detailed scientific investigation has not been carried out in the past. Magyar et al. [23] conducted drilling experiments in BFRP composites and analysed the influences of process parameters on the drilling-induced burr and microstructure. They showed that the cutting speed has the most significant influence on surface roughness, and the effect of the feed is negligible. At the same time, the feed was found as the most significant factor affecting the size of burrs.

Thrust force in the drilling of carbon fibre-reinforced polymer (CFRP) composites was investigated and modelled by many scholars. Phapale et al. [24] developed a finite element (FE) model for the prediction of critical thrust force in CFRPs and validated it with experimental results. The prediction accuracy of their FE model was within 5%. Bai et al. [25] proposed a novel mechanical model for predicting thrust force with the consideration of tool wear in CFRPs. Their model provided better predictions (within 14%) than the analysed empirical methods. Zhang et al. [26] developed a theoretical model for predicting of thrust force in the drilling of CFRP stacks. The influence of tool wear was also considered in their model. They found the average absolute relative error of their model within 9%. Luo et al. [27] presented a mechanistic thrust force model in the drilling of CFRP/Ti stacks. The adequacy of their model is good, *i.e.* average prediction error was found to be below 10%. Wang et al. [28] developed a thrust force prediction method in the drilling of CFRPs. They considered the effect of the orientation angle, namely the angle between the cutting edge (chisel edge) and fibre direction. Although they did not provide numerical information on the prediction accuracy of their model, their results seem to be promising.

Although there are some published experiences in the drilling of BFRP composites, the analysis and modelling of cutting force in the drilling of BFRPs are not conducted yet. Considering that the thrust force has a key role in drilling-induced geometrical defect (*e.g.* delamination) formations in fibrous composites [17, 29], the main aim of this paper is to model the thrust force during the drilling of BFRP composites. Two modelling methods were used to develop cutting force models. In order to calculate the regression coefficients and model parameters, and to validate the adequacy of the developed models, mechanical drilling experiments were performed according to the experimental setup presented in Sect. 2. Then, the results are presented and discussed in Sect. 3.

2 Experimental setup and methods

2.1 Materials, tools, and machines

A unidirectional carbon fibre-reinforced vinyl-ester-based polymer composite and a multidirectional (biaxial) basalt fibre-reinforced epoxy resin-based polymer (MD-BFRP) composite were drilled in the drilling experiments. Our industrial partner provided both composites, as they plan to replace their CFRP components with the more sustainable BFRP composite. The main material properties of the composites were measured and published in our previous study [23].

A Kondia B640 three-axis machining centre was used to perform the drilling experiments. The experiments were carried out in a dry environment, where a Nilfisk GB733 industrial vacuum cleaner provided the chip extraction. A titanium–aluminium-coated Ø10 mm Tivoly Polaris 150 Sim Dim 6537 K solid carbide drill was used to perform the drilling. The tool geometry is based on the DIN 6537 k standard. The tool has a point angle of 145°, a helix angle of 35°, and a chisel edge length of 1 mm. The composites were fixed by a special fixture providing identical supporting circumstances on the entry and exit sides.

A KISTLER 9257BA three-component dynamometer was applied to measure the cutting force in situ using a 10 000-Hz sampling frequency. A KISTLER 5070 multi-channel charge amplifier and two National Instruments USB-4431 dynamic signal acquisition modules were used for force data sampling. The tool condition was documented by capturing microscopic images on the cutting edges before, between, and after the experiments using a Dino-Lite AM413ZT digital microscope. The experimental machining setup can be seen in Fig. 1a.

Considering that the expected interaction terms may be significant and the expected influences of the process parameters are often nonlinear, the continuous factors are

Fig. 1 Illustration of the, **a** experimental machining setup and **b** geometric representation of the CCF experimental design, where x_1 and x_2 denote the factors (independent variables) and the points represent the experimental setups considering that the middle point (5th) is repeated five times to gather information on the variances
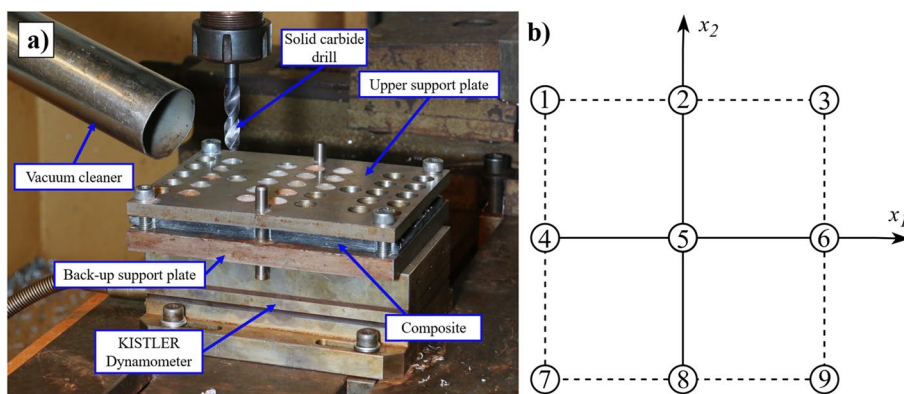
Table 1 Factor levels

Factor	Levels		
	−1	0	1
Material type (−)		BFRP	CFRP
Cutting speed (m/min)	50	100	150
Feed (mm/rev)	0.05	0.10	0.15

recommended to be varied at least three levels. To gather helpful information on the properties of the composites in machining with relatively few drilling operations, the central-composite face-centred (CCF) design of experiments was used, which geometrical representation is illustrated in Fig. 1b. The composite type as a categorical factor with two levels (BFRP and CFRP) and the feed (mm/rev) and cutting speed (m/min) as continuous factors, each on three different levels, were varied according to the experimental table as is shown in Table 2. The levels of these continuous factors (Table 1) were defined based on previous studies and the recommendations of the tool manufacturers [7, 23, 30, 31]. The experimental design is suitable for the application of quadratic models to describe nonlinear influences of process parameters. The drilling operations were performed in a randomised order, and settings of level zero ($v_c = 100$ m/min, $f = 0.10$ mm/rev) were repeated five times, which enabled us to determine the reproducibility and calculate the variances. The analysis of variances (ANOVA) was performed at a significance level of $\alpha = 0.05$.

2.2 Methods

The raw data of the measured force were processed by a self-developed algorithm in Python to handle quickly, slice, filter, and evaluate the data and characterise the process. The evaluation process is automated; only the start and the end point of the useful data have to be defined manually. First, the code slices the data as defined by the user. Then, a Butterworth low-pass filter at a cut-off frequency of 300 Hz

(approx. five four the frequency of the maximal spindle speed to include harmonics frequencies) was used in order to filter the high-frequency noises as shown in Fig. 2. Filtering the raw force data measured during machining experiments is necessary to remove interfering high-frequency vibrations from the experimental environment that are irrelevant to the test object. This results in a smoothed data series, better suited to the nature of the machining operation, from which the metrics describing the processes (*e.g.* thrust force) can be more accurately determined. The F_z denotes the filtered axial cutting force component at a constant chip cross section. Then, the thrust force (F_t) is calculated according to **Eq.** (1). Considering that the larger the F_z, the less beneficial the drilling process is from the point of view of tool wear and hole quality, the maximum of F_z (*i.e.* F_t) is selected to characterise the process. The recorded and processed cutting force is illustrated in Fig. 2.

$$F_t = max\left(F_{zi}\right), i = 0, 1 \ldots n \tag{1}$$

First, response surface methodology (RSM) was used to statistically model the thrust force of the drilling process. According to previous investigations [32–36], the effects of the applied process parameters on the thrust force are expected to be nonlinear; therefore, a second-degree polynomial model was used, as expressed by **Eq.** (2).

$$F_t(x_1, x_2 \ldots x_n) = b_0 + \sum_{i=1}^{n} b_i x_i + \sum_{i=1}^{n} b_{ii} x_{ii}^2 + \sum_{i=1}^{n-1} \sum_{j=i+1}^{n} b_{ij} x_i x_j + \delta \tag{2}$$

where F_t is the corresponding response value (*i.e.* thrust force), x_i are the factors (*i.e.* feed and cutting speed), b_0, b_i, b_{ij}, and b_{ii} are the regression coefficients of the parameters, and δ is a random experimental error. Then, the significance of the factors and their interactions were determined through the analysis of variance (ANOVA) technique at a significance level of $\alpha = 0.05$.

Second, the F_z was modelled through advanced statistics considering the actual cutting tool edge position and feed,

as expressed by **Eq.** (3). The applied advanced statistical model takes account of the symmetry observed in the structure of the material and therefore uses a periodic function. Furthermore, it was important that the function should be differentiable and computable easily, providing the possibility of real-time process monitoring for future industrial applications.

$$F_z(\varphi) = A \bullet \sin\left(\omega^{-1} \bullet \varphi + \Delta\right) + k \tag{3}$$

where φ (°) denotes the angular position of the spindle, $\omega = 2\pi n/60$ (rad/s) is the angular frequency of the spindle; moreover, A, Δ and k are regression coefficients denoting amplitude, phase shift and vertical shift, respectively. Considering that the advanced model includes the effect of φ, which is closely correlated with the fibre cutting angle, this model is able to predict not only the thrust force but also the axial cutting force tool. In addition, as the feed has a significant statistical and physical influence on the cutting force, we implemented it in our model, as expressed by **Eq.** (4).

$$F_z(\varphi, f) = C \bullet F_z(\varphi) \bullet f^x \tag{4}$$

where f (mm/rev) denotes the feed; moreover, C and x are regression coefficients used to model the effect of the feed. The thrust force (F_t) can be predicted through the maximum of **Eq.** (4), as expressed by **Eq.** (5).

$$F_t(\varphi, f) = max\left(F_z(\varphi, f)\right) \tag{5}$$

The coefficient of determination (R^2) was used to determine the adequacy of the model fitting as it is a widely used measure to describe how well a statistical model can predict the outcome of a phenomenon, which is the thrust force in this study. The absolute percentage error (APE) was used to characterise the adequacy of the F_t predictions, as expressed by **Eq.** (6).

$$APE = abs\left(\frac{F_{t,p} - F_{t,m}}{F_{t,m}}\right) \bullet 100 \tag{6}$$
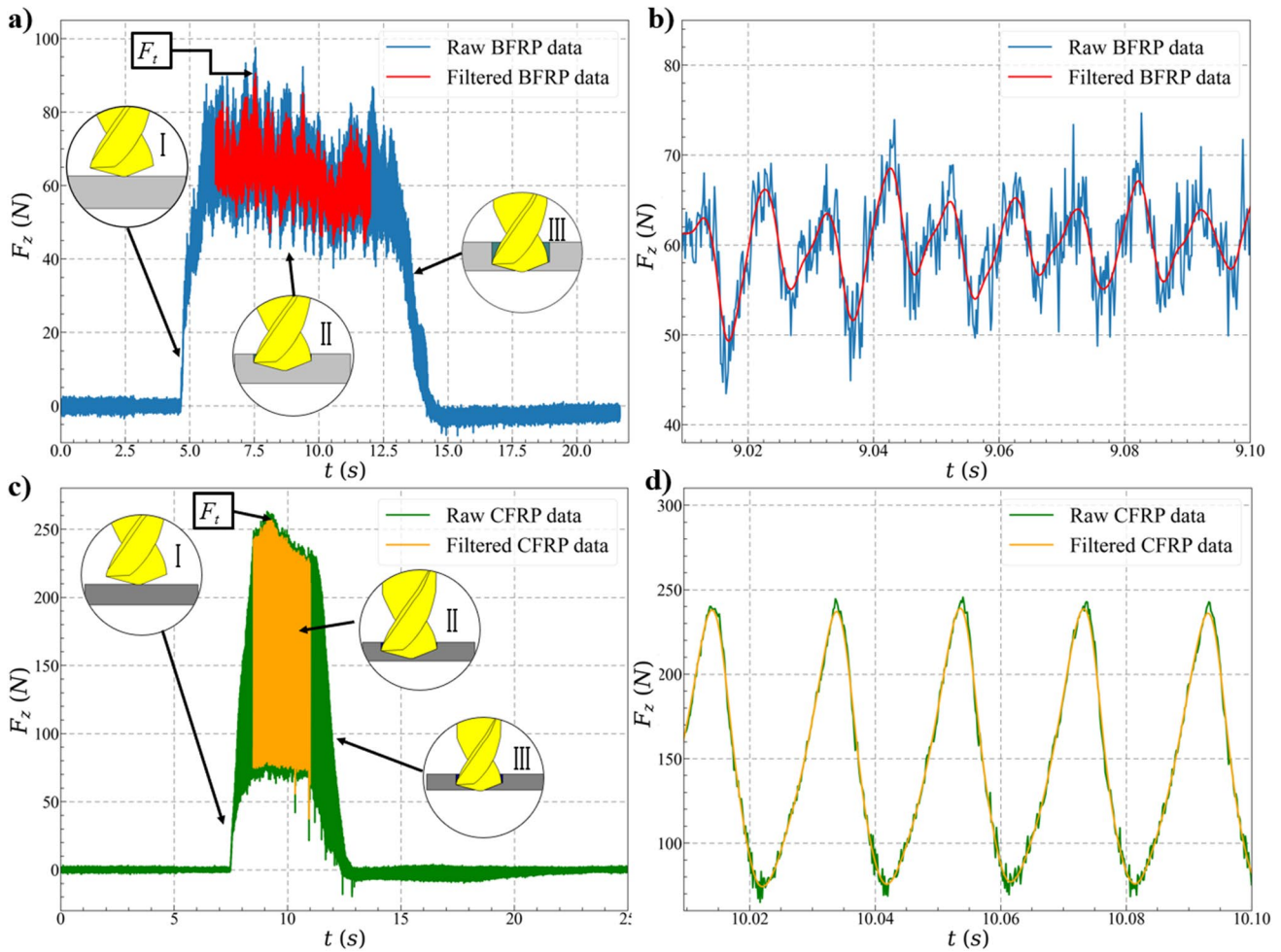

Fig. 2 Illustration of the workflow of the thrust force (F_t) generation: **a** raw dataset (blue), and the trimmed and filtered (red) force signal of BFRP (F_z), **b** enlarged part of the raw dataset and F_z of BFRP, **c** raw dataset (green), and the trimmed and filtered (orange) force signal of CFRP (F_z), **d** enlarged part of the raw dataset and F_z of CFRP

3 Results and discussion

This section presents the developed models, the predictions, and their comparison and discussion. The measured and predicted thrust forces and the adequacy of models are summarised in Table 2 and discussed separately in the following subsections.

Representative filtered force diagrams of BFRP and CFRP composites are shown in Fig. 3. Force diagrams clearly show that the BFRP composite has much smoother characteristics (Fig. 3a), while the CFRP composite shows a higher-amplitude characteristic (Fig. 3b). This difference is resulted by the different reinforcement structures of the composites. The BFRP composite with a biaxial reinforcement results in a relatively more anisotropy structure compared to CFRP with a UD reinforcement, which explains why the thrust force diagrams of the BFRP composite show a much more flattened shape. Furthermore, it can also be observed that the thrust force (F_t) was much larger for the CFRP composite (Table 2), as was expected based on the strength tests [23]. The diagrams also indicate that the smaller the feed, the longer the operation time, as it was expected.

3.1 RSM models

The developed thrust force prediction models based on the RSM for BFRP and CFRP composites are expressed by **Eq.** (7) and **Eq.** (8), respectively. The response surface diagrams (graphical illustrations of the RSM models) are illustrated in Fig. 4. These diagrams represent the effect of the technological parameters (*i.e.* feed and cutting speed) on the thrust force. The averages of the absolute percentage errors are 3.26% and 3.03% for the BFRP and CFRP composites, respectively. These errors are within the scope of mechanical engineering and manufacturing science expectations, thus proving their applicability.

$$F_{t,RSM}^{BFRP} = 20.6 + 1536f - 0.054v_c - 4980f \bullet f + 0.001v_c \bullet v_c - 0.71f \bullet v_c \tag{7}$$

$$F_{t,RSM}^{CFRP} = 158.3 + 2284f - 0.066v_c - 4980f \bullet f + 0.001v_c \bullet v_c - 0.71f \bullet v_c \tag{8}$$

The combination of *F*-values and *P*-values is examined to determine whether the factors and their interactions have a significant effect on the thrust force. The applied null hypothesis is that the influence of the x_1 factor on the *Y* response parameter is not significant considering the given significance level. In the case where the *P*-value is greater than $\alpha = 0.05$, the null hypothesis is failed to be rejected, meaning that the particular effect will not be considered to be significant. The response graphs suggest that the influence of the cutting speed is negligible. This is in a good correlation to the ANOVA results, as the *P*-value of the cutting speed is large (*P*-value = 0.416), as Table 3 shows. Furthermore, it can be seen that the influence of the feed on the thrust force is significant, as significantly larger force values are belonging to the larger feed levels. The interaction effect of the feed and cutting speed is not significant (*F*-value = 0.12; *P*-value = 0.734), as the influence of feed is not affected by the level of cutting speed in the analysed factor space. This is proved by the ANOVA table (Table 3). Based on the results of the ANOVA, the type of the composite has by far the most significant (*F*-value = 1626.12 *P*-value = 0.000) effect on the thrust force, followed by the feed (*F*-value = 104.49; *P*-value = 0.000).

The main effect plots of the significant factors can be seen in Fig. 5. The diagrams show that the composite type has the most significant influence on the cutting force, *i.e.* the thrust force in the BFRP composites is significantly lower than that of CFRPs (Fig. 5a). This may be due to the stronger (*i.e.* tensile, interlaminar, impact) carbon fibrous polymer composites than basalt fibrous polymer composites [23]. Figure 5b indicates that the larger the feed, the larger the thrust force in each composite. This was expected because the larger the feed, the larger the chip cross section and the larger the cutting force is [37, 38].

Although the developed RSM models predict accurately (APE is below 11%) the value of thrust force at different levels of feed and cutting speed and may be used for real-time process control—as the polynomial form of the model makes it easy and fast to calculate with—these are not describing the nature of the axial cutting force (F_z) component. Considering that these RSM models fail to represent the influences of fibres on the cutting force, an advanced statistical method was required to be developed, as presented in Sect. 2.2 and Sect. 3.2.

3.2 Advanced statistical models

Considering that the fibre cutting angle (*i.e.* the angle between the fibre and cutting speed direction) continuously changes, the filtered thrust force data are sinusoidal (shown in Fig. 2b and Fig. 2d). Thus, we fitted a sinusoidal function to the filtered datasets to model the characteristics of each force diagram. Furthermore, the influence of the feed is also added to the advanced model, as it was found to have a significant influence on the thrust force. The model coefficients were calculated through the least squares method. The developed advanced statistical models to predict F_z are expressed by **Eq.** (9) and **Eq.** (10) for the BFRP and CFRP composites, respectively.

Table 2 Experimental design table containing the measured values of the thrust force (F_t) with the predictions obtained by the RSM model ($F_{t,RSM}$) and the advanced statistical method ($F_{t,adv}$), along with the absolute percentage error of both models, and the R^2 predictions belonging to the F_z predictions achieved by the advanced statistical models

No	Factors		BFRP						CFRP					
			Measured	Predicted		APE		R^2	Measured	Predicted		APE		R^2
	f (mm/rev)	v_c (m/min)	F_t (N)	$F_{t,RSM}$ (N)	$F_{t,adv}$ (N)	$F_{t,RSM}$ (%)	$F_{t,adv}$ (%)	(-)	F_t (N)	$F_{t,RSM}$ (N)	$F_{t,adv}$ (N)	$F_{t,RSM}$ (%)	$F_{t,mech}$ (%)	(-)
1	0.05	50	90.85	82.98	94.85	8.67	4.40	0.768	256.60	257.48	252.49	0.34	1.60	0.962
2	0.15	100	138.54	132.90	144.07	4.07	3.99	0.619	385.82	381.60	380.77	1.09	1.31	0.974
3	0.15	50	131.89	133.43	161.88	1.16	22.73	0.807	344.94	381.60	380.77	10.63	10.39	0.732
4	0.10	100	121.48	121.90	123.48	0.35	1.65	0.627	336.52	333.20	327.20	0.99	2.77	0.978
5	0.10	100	122.60	121.90	123.48	0.57	0.71	0.634	338.94	333.20	327.20	1.69	3.47	0.972
6	0.10	100	115.50	121.90	123.48	5.54	6.90	0.622	340.69	333.20	327.20	2.20	3.96	0.976
7	0.10	150	124.28	128.15	123.48	3.11	0.65	0.530	347.90	338.85	327.20	2.60	5.95	0.891
8	0.15	150	141.99	137.38	144.07	3.25	1.47	0.445	406.12	382.73	380.77	5.76	6.24	0.370
9	0.10	50	113.16	120.65	123.48	6.62	9.12	0.803	311.12	332.55	327.20	6.89	5.17	0.746
10	0.05	100	89.08	86.00	94.85	3.46	6.48	0.879	259.26	267.33	252.49	3.11	2.61	0.959
11	0.05	150	91.92	94.03	94.85	2.28	3.19	0.764	267.12	267.33	252.49	0.08	5.48	0.514
12	0.10	100	119.17	121.90	123.48	2.29	3.62	0.630	339.23	333.20	327.20	1.78	3.55	0.976
13	0.10	100	123.53	121.90	123.48	1.32	0.04	0.650	340.92	333.20	327.20	2.26	4.03	0.977

Fig. 3 Representative filtered force diagrams of **a** BFRP and **b** CFRP composites at a cutting speed of $v_c = 100$ m/min
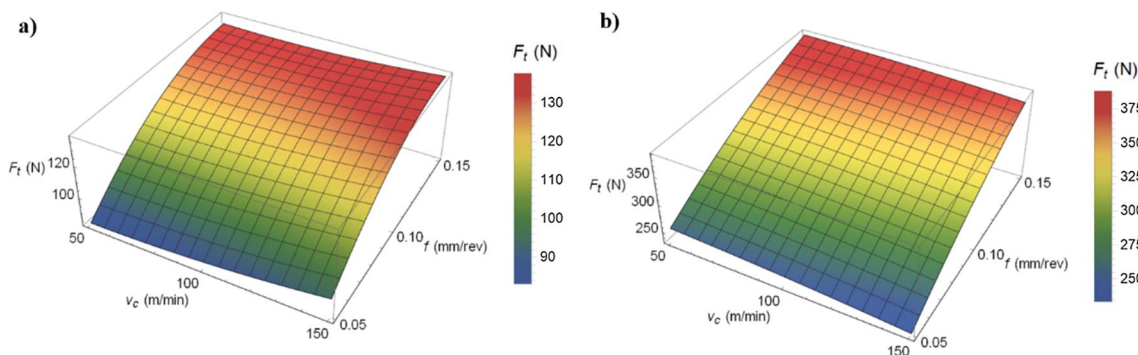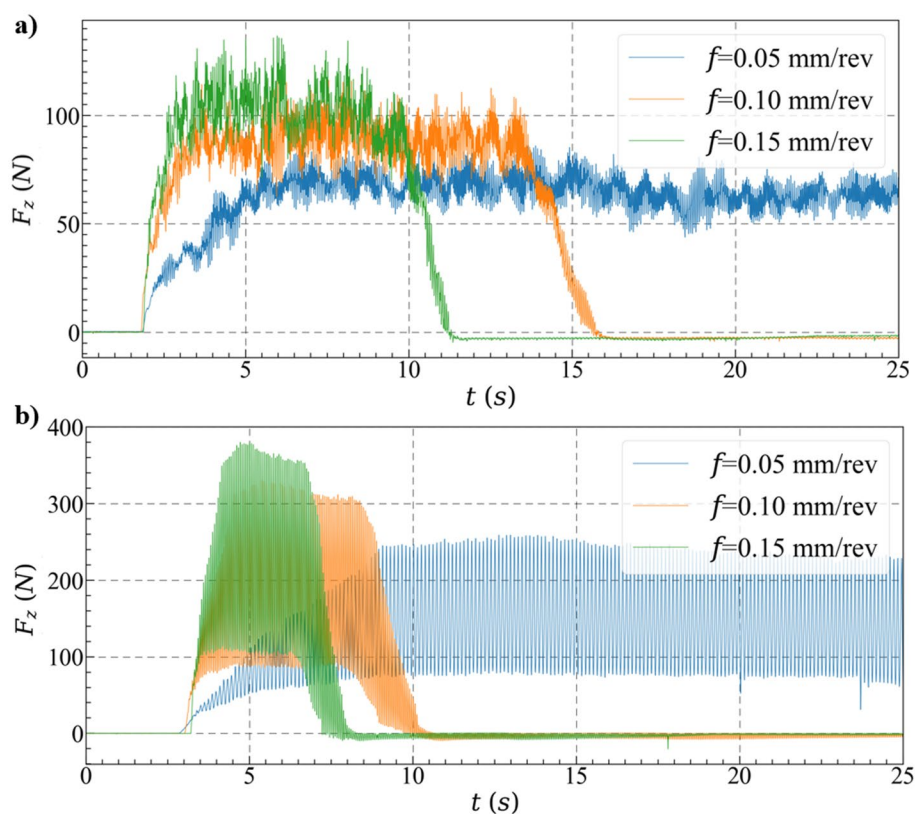

Fig. 4 The effect of technological parameters (f and v_c) on the thrust force (F_t) at drilling **a** BFRP and **b** CFRP composites using RSM models

$$F_{z,adv}^{BFRP}(\varphi, f) = 2.4546 \bullet (50.5881 \bullet$$
$$\sin(0.0347 \bullet \varphi + 0.0000) + 85.1331) \bullet f^{0.3804} \tag{9}$$

$$F_{z,adv}^{CFRP}(\varphi, f) = 2.4178 \bullet (102.6220 \bullet$$
$$\sin(0.0347 \bullet \varphi + 0.5629) + 180.6572) \bullet f^{0.3739} \tag{10}$$

In the case of these advanced statistical models, the averages of the absolute percentage error of the calculated thrust forces (*i.e.* the maximums of **Eq.** (9) and **Eq.** (10)) are 4.99% and 4.35% for the BFRP and CFRP composites, respectively.

Although these average *APE*s are slightly larger than the *APE*s found in the RSM models, these errors are still within the scope of mechanical engineering and manufacturing science expectations. In addition, these advanced models are capable of predicting not only the maximums of the F_z, but also its characteristics, as it is illustrated in Fig. 6, where the best fitting sections of the whole force dataset are shown. While the diagrams qualitatively indicate that the advanced models fit well the measured and filtered force dataset, the averages of the coefficient of determination (R-squared) values of 0.6751 and 0.8481 indicate the adequacy of the fitting

Table 3 The result of ANOVA in the case of thrust force

Source	DF	Adj SS	Adj MS	F value	P value
Model	8	316,300	39,538	226.59	0.000
Linear	3	300,800	100,267	574.64	0.000
f	1	18,232	18,232	104.49	**0.000**
v_c	1	121	121	0.70	0.416
composite	1	283,737	283,737	1626.12	**0.000**
Square	2	870	435	2.49	0.112
$f \cdot f$	1	831	831	4.76	0.043
$v_c \cdot v_c$	1	29	29	0.17	0.690
Two-way interaction	3	3883	1294	7.42	0.002
$f \cdot v_c$	1	21	21	0.12	0.734
$f \cdot composite$	1	3594	3594	20.60	**0.000**
$v_c \cdot composite$	1	1	1	0.01	0.940
Error	17	2966	174		
Lack-of-fit	7	2046	292	3.18	0.048
Pure error	10	920	92		
Total	25	319,267			

Bold entries denote *P*-values lower than 0.05, indicating that the particular factor has a significant effect
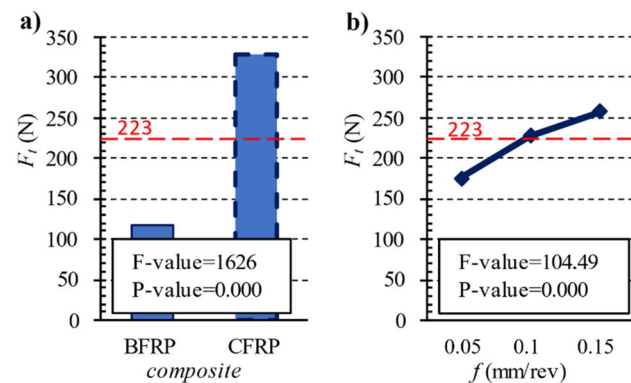
Fig. 5 Main effect plots of the **a** type of the composite and **b** the feed

of the models in the case of BFRP and CFRP composites, respectively.

3.3 Comparison and discussion

The absolute percentage errors of the developed RSM models indicate that the prediction of the thrust force (F_t) is accurate; thus, these models can be applied for thrust force modelling and drilling process optimisation. Considering that the RSM models are polynomial, these models can be efficiently used in real-time (*i.e.* in situ) process diagnostics and monitoring of drilling CFRP and BFRP composites because polynomial calculations do not require a significant amount of computational capacity. In

addition, these models can be implemented in Industry 4.0-driven digital-twin models too. Although the thrust force is accurately predicted by these RSM models, they provide no in-depth understanding of the machining mechanisms, *i.e.* does not include the mechanistic effect of fibre cutting angle, chip cross section. Consequently, another drawback of these RSM models is that only the maximum axial cutting force (*i.e.* thrust force) can be predicted and not the characteristics of the axial cutting force component. In order to further improve these models, the effect of the feed at more levels is recommended to be analysed to increase the performance of the models.

Advanced statistical models—compared with the RSMs—predict not only the thrust force but the $F_z(\phi)$ function also. Although the absolute percentage errors of these advanced models are slightly larger than those of the RSM models, these can be applied to analyse the characteristics of the axial cutting force in the drilling of CFRP and BFRP composites. The regression coefficients (R^2) of the advanced models are 0.6751 and 0.8481 for the BFRP and CFRP, respectively. The R^2 of the CFRP composite model is in the range achieved by similar research works [37, 39–42]; thus, it is accurate enough to use. Although the method for the model building of the BFRP and CFRP composites is identical, the R^2 of the BFRP becomes significantly smaller than that of CFRPs. However, in the case of advanced statistical models, there are opportunities to improve the fit to the measured datasets. This may require the development of more complex models, which might complicate the application in real industry scenarios due to the high computational demand. Nevertheless, there are no existing similar results published to prove the adequacy of this prediction, according to the best knowledge of the authors.

The experimental results show that the thrust force is significantly lower in the BFRP than in the CFRP composite. Considering that the lower the thrust force, the lower the tool wear rate is [25], the tool wear speed is expectedly lower in the BFRPs than expected in the CFRP composites. However, this has to be proved by further investigations. In addition to the beneficial ability of BFRPs to have low thrust forces, the sustainability of natural basalt fibres-reinforced polymer composites is larger than that of CFRPs. Therefore, if the mechanical properties of a BFRP composite part are suitable for replacing existing CFRP parts, it is recommended to use the BFRP composites from the point of view of drilling.

Considering that the dominancy of the ploughing phenomena is significantly more decisive when microholes (diameter less than 1 mm) are drilled, the findings of the current study are valid only conventional-sized dry drilling of BFRP and CFRP composites. Therefore, the analysis of the influences of the cutting tool diameter and machining conditions (*e.g.* cooling techniques, mechanical supporting circumstances of composite plies, application of support
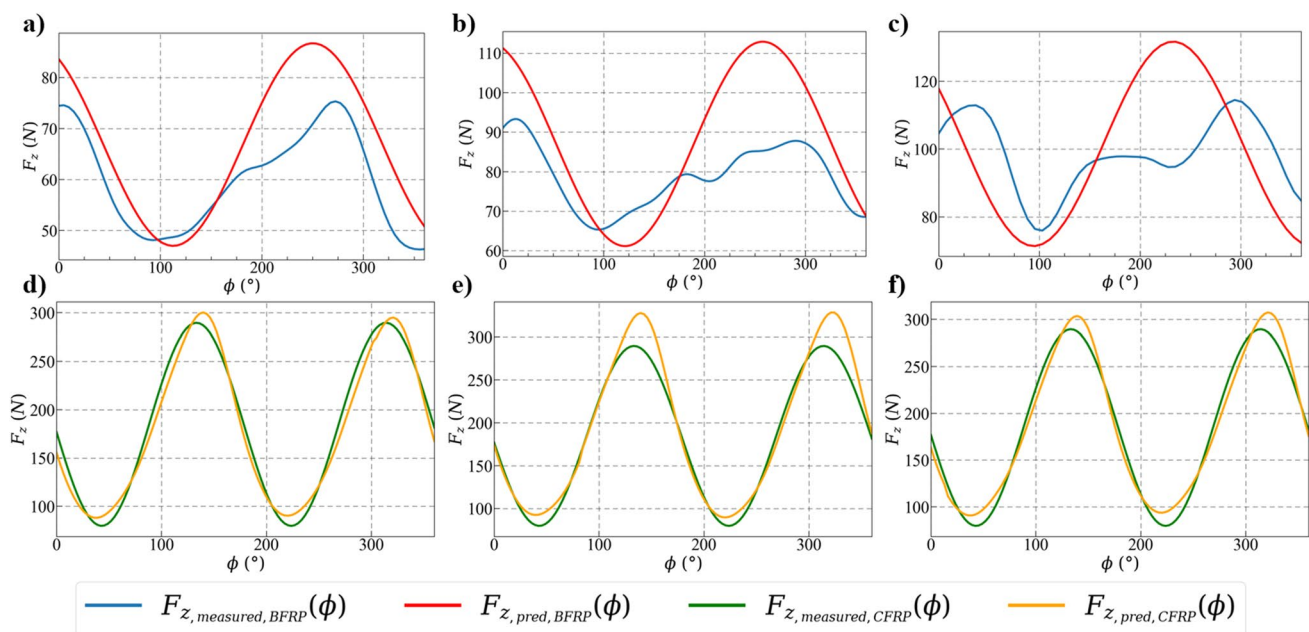
Fig. 6 Illustration of the fitting of the prediction models to the measured and filtered cutting forces in **a–c** BFRP and **d–f** CFRP composites

plates, application of tool vibration and laser assistance) is required in the future.

Although the authors experienced similar chip removal, axial force generation, and similar effects of drilling parameters when drilling BFRP composites compared to the CFRPs, the in-depth analysis of chip removal mechanisms and tool wear mechanisms in the machining of BFRPs is recommended to support the spread of BFRP applications in the future. As the number and depth of similar research works are moderate, this study directly supports the current trends in sustainable material usage in high-end industries.

4 Conclusions

In the present study, mechanical drilling experiments were conducted in basalt and carbon fibre-reinforced polymer (BFRP and CFRP) composites and the thrust force was modelled through response surface methodology and advanced statistics. According to the present study, the following conclusions can be drawn:

- Response surface methodology (RSM) models were developed to describe the influences of process parameters on the thrust force in drilling BFRP and CFRP composites. The averages of the absolute percentage errors of the RSM models are 3.26% and 3.03% for the BFRP and CFRP composites, respectively. These models include the effect of feed (mm/rev) and cutting speed (m/min).

- The analysis of variances (ANOVA) results prove that the type of the composite has by far the most significant effect on the thrust force (whether it is BFRP or CFRP), followed by the feed. The influence of the cutting speed is negligible on the thrust force. The larger the feed, the larger the thrust force in each composite. Furthermore, the thrust force in the BFRP composites was significantly lower than that of CFRPs.

- We fitted a sinusoidal function to the filtered datasets to model the characteristics of each force diagram. This model includes the influence of the angular position of the cutting tool and the feed. The averages of the absolute percentage error of the calculated thrust forces are 4.99% and 4.35% for the BFRP and CFRP composites, respectively. Thus, this sinusoidal model is suitable for modelling the thrust force in the drilling of BFRP composites.

- This experimental study suggests that if the mechanical properties of a BFRP composite part are suitable for replacing an existing CFRP part, it is recommended to use the BFRP composites from the point of view of drilling.

Although the machining behaviour of BFRPs seems to not differ significantly from that of CFRPs, further research works are recommended to support the spread of BFRP applications, *i.e.* an in-depth analysis of chip removal mechanisms and tool wear mechanisms in the machining of BFRPs.

Author contributions GM helped in resources, investigation, formal analysis, visualization, software, writing—original draft; NG was involved in conceptualization, methodology, writing—review & editing, supervision.

Code availability Not applicable.

Declarations

Conflicts of interest Not applicable.

Ethics approval Not applicable.

Consent to participate Not applicable.

Consent for publication Not applicable.

References

1. Geier N, Paulo Davim J, Szalay T (2019) Advanced cutting tools and technologies for drilling carbon fibre reinforced polymer (CFRP) composites: a review. Compos Part A Appl Sci Manuf 125:105552. https://doi.org/10.1016/j.compositesa.2019.105552

2. István Poór D, Geier N, Pereszlai C, Xu J (2021) A critical review of the drilling of CFRP composites: burr formation, characterisation and challenges. Compos Part B Eng. https://doi.org/10.1016/j.compositesb.2021.109155

3. Xu J, Yin Y, Paulo Davim J et al (2022) A critical review addressing drilling-induced damage of CFRP composites. Compos Struct 294:115594. https://doi.org/10.1016/j.compstruct.2022.115594

4. Forintos N, Czigany T (2019) Multifunctional application of carbon fiber reinforced polymer composites: electrical properties of the reinforcing carbon fibers—A short review. Compos B Eng 162:331–343. https://doi.org/10.1016/j.compositesb.2018.10.098

5. Altin Karataş M, Gökkaya H (2018) A review on machinability of carbon fiber reinforced polymer (CFRP) and glass fiber reinforced polymer (GFRP) composite materials. Def Technol. https://doi.org/10.1016/j.dt.2018.02.001

6. Geier N, Poór DI, Pereszlai C et al (2022) A drilling case study in polymer composites reinforced by virgin and recycled carbon fibres (CFRP and rCFRP) to analyse thrust force and torque. Int J Adv Manuf Technol. https://doi.org/10.1007/s00170-022-08947-1

7. Geier N, Poór DI, Pereszlai C, Tamás-Bényei P (2022) Drilling of recycled carbon fibre–reinforced polymer (rCFRP) composites: analysis of burrs and microstructure. Int J Adv Manuf Technol. https://doi.org/10.1007/s00170-022-08847-4

8. Balaji AB, Rudd C, Liu X (2020) Recycled carbon fibers (rCF) in automobiles: towards circular economy. Mater Circ Econ 2:4. https://doi.org/10.1007/s42824-020-00004-0

9. Czigány T, Vad J, Pölöskei K (2005) Basalt fiber as a reinforcement of polymer composites. Period Polytech Mechan Eng 49:3–14

10. Czigány T (2006) Special manufacturing and characteristics of basalt fiber reinforced hybrid polypropylene composites: mechanical properties and acoustic emission study. Compos Sci Technol 66:3210–3220. https://doi.org/10.1016/j.compscitech.2005.07.007

11. Colombo C, Vergani L, Burman M (2012) Static and fatigue characterisation of new basalt fibre reinforced composites. Compos Struct 94:1165–1174. https://doi.org/10.1016/j.compstruct.2011.10.007

12. Ross A (2006) Basalt fibers: alternative to glass? Compos Technol 12:44–48

13. Zhang H, Yao Y, Zhu D et al (2016) Tensile mechanical properties of basalt fiber reinforced polymer composite under varying strain rates and temperatures. Polym Test 51:29–39. https://doi.org/10.1016/j.polymertesting.2016.02.006

14. Altalmas A, El Refai A, Abed F (2015) Bond degradation of basalt fiber-reinforced polymer (BFRP) bars exposed to accelerated aging conditions. Constr Build Mater 81:162–171. https://doi.org/10.1016/j.conbuildmat.2015.02.036

15. Amuthakkannan P, Manikandan V, Uthayakumar M (2015) Analysis of delamination in drilling of basalt fiber reinforced polymer composites. Mater Phys Mech 24:1–8

16. Abhishek K, Datta S, Mahapatra SS (2015) Optimization of thrust, torque, entry, and exist delamination factor during drilling of CFRP composites. Int J Adv Manuf Technol 76:401–416. https://doi.org/10.1007/s00170-014-6199-3

17. Abrão AM, Rubio JCC, Faria PE, Davim JP (2008) The effect of cutting tool geometry on thrust force and delamination when drilling glass fibre reinforced plastic composite. Mater Des 29:508–513. https://doi.org/10.1016/j.matdes.2007.01.016

18. Aveen KP, Londe NV, Amin GG, Salim Shaikh I (2021) A review on the effects of input parameters & filler composition on delamination during machining of FRP composites. Mater Today Proceed 46:2607–2611. https://doi.org/10.1016/j.matpr.2021.02.264

19. Davim JP, Rubio JC, Abrao AM (2007) A novel approach based on digital image analysis to evaluate the delamination factor after drilling composite laminates. Compos Sci Technol 67:1939–1945. https://doi.org/10.1016/j.compscitech.2006.10.009

20. Navarro MD, Meseguer MD, Sánchez A, Gutiérrez S (2017) Tool wear study in edge trimming on basalt fibre reinforced plastics. Procedia Manuf 13:259–266. https://doi.org/10.1016/j.promfg.2017.09.067

21. Navarro-Mas MD, García-Manrique JA, Meseguer MD et al (2018) Delamination study in edge trimming of basalt fiber reinforced plastics (BFRP). Materials. https://doi.org/10.3390/ma11081418

22. Navarro-Mas M, Meseguer M, Lluch-Cerezo J, Garcia-Manrique J (2020) Comparison of different parameters to evaluate

delamination in edge trimming of basalt fiber reinforced plastics (BFRP). Materials 13:5326. https://doi.org/10.3390/ma13235326

23. Magyar G, Károly D, Xu J, Geier N (2022) Analysis of drilling-induced geometrical damages in basalt and carbon fibre-reinforced polymer (BFRP and CFRP) composites. Int J Adv Manuf Technol. https://doi.org/10.1007/s00170-022-10173-8

24. Phapale K, Ahire A, Singh R (2018) Experimental characterization and finite element modeling of critical thrust force in cfrp drilling. Mach Sci Technol 22:249–270. https://doi.org/10.1080/10910344.2017.1337134

25. Bai Y, Jia Z, Fu R et al (2021) Mechanical model for predicting thrust force with tool wear effects in drilling of unidirectional CFRP. Compos Struct 262:113601. https://doi.org/10.1016/j.compstruct.2021.113601

26. Zhang Y, Wu D, Chen K (2019) A theoretical model for predicting the CFRP drilling-countersinking thrust force of stacks. Compos Struct 209:337–348. https://doi.org/10.1016/j.compstruct.2018.10.107

27. Luo B, Li Y, Zhang K et al (2015) A novel prediction model for thrust force and torque in drilling interface region of CFRP/Ti stacks. Int J Adv Manuf Technol 81:1497–1508. https://doi.org/10.1007/s00170-015-7294-9

28. Wang D, Jiao F, Mao X (2020) Mechanics of thrust force on chisel edge in carbon fiber reinforced polymer (CFRP) drilling based on bending failure theory. Int J Mech Sci 169:105336. https://doi.org/10.1016/j.ijmecsci.2019.105336

29. Geng D, Liu Y, Shao Z et al (2019) Delamination formation, evaluation and suppression during drilling of composite laminates: A review. Compos Struct 216:168–186. https://doi.org/10.1016/j.compstruct.2019.02.099

30. Geier N, Szalay T (2017) Optimisation of process parameters for the orbital and conventional drilling of uni-directional carbon fibre-reinforced polymers (UD-CFRP). Measurement 110:319–334. https://doi.org/10.1016/j.measurement.2017.07.007

31. Davim JP, Reis P (2003) Study of delamination in drilling carbon fiber reinforced plastics (CFRP) using design experiments. Compos Struct 59:481–487. https://doi.org/10.1016/S0263-8223(02)00257-X

32. Karpat Y, Polat N (2013) Mechanistic force modeling for milling of carbon fiber reinforced polymers with double helix tools. CIRP Ann 62:95–98. https://doi.org/10.1016/j.cirp.2013.03.105

33. Masek P, Zeman P, Kolar P, Holesovsky F (2019) Edge trimming of C/PPS plates. Int J Adv Manuf Technol 101:157–170. https://doi.org/10.1007/s00170-018-2857-1

34. Czampa M, Biro I, Szalay T (2017) Effects of different cutting conditions on the surface roughness parameters of iron-copper-carbon powder metallurgy composites. Int J Mach Mach Mater 19:440–456. https://doi.org/10.1504/IJMMM.2017.087617

35. Jáuregui JC, Reséndiz JR, Thenozhi S et al (2018) Frequency and time-frequency analysis of cutting force and vibration signals for tool condition monitoring. IEEE Access 6:6400–6410. https://doi.org/10.1109/ACCESS.2018.2797003

36. Balázs BZ, Takács M (2020) Experimental investigation and optimisation of the micro milling process of hardened hot-work tool steel. Int J Adv Manuf Technol 106:5289–5305. https://doi.org/10.1007/s00170-020-04991-x

37. Anand RS, Patra K (2017) Mechanistic cutting force modelling for micro-drilling of CFRP composite laminates. CIRP J Manuf Sci Technol 16:55–63. https://doi.org/10.1016/j.cirpj.2016.07.002

38. Xu J, An Q, Chen M (2014) A comparative evaluation of polycrystalline diamond drills in drilling high-strength T800S/250F CFRP. Compos Struct 117:71–82. https://doi.org/10.1016/j.compstruct.2014.06.034

39. Li S, Dai L, Li C et al (2022) Prediction model of chisel edge thrust force and material damage mechanism for interlaminar-direction drilling of UD-CFRP composite laminates. Compos Struct 298:116023. https://doi.org/10.1016/j.compstruct.2022.116023

40. Pereszlai C, Geier N, Poór DI et al (2021) Drilling fibre reinforced polymer composites (CFRP and GFRP): an analysis of the cutting force of the tilted helical milling process. Compos Struct 262:113646. https://doi.org/10.1016/j.compstruct.2021.113646

41. Geier N, Szalay T, Takács M (2018) Analysis of thrust force and characteristics of uncut fibres at non-conventional oriented drilling of unidirectional carbon fibre-reinforced plastic (UD-CFRP) composite laminates. Int J Adv Manuf Technol 100:3139–3154. https://doi.org/10.1007/s00170-018-2895-8

42. Song Y, Cao H, Zheng W et al (2022) Cutting force modeling of machining carbon fiber reinforced polymer (CFRP) composites: a review. Compos Struct 299:116096. https://doi.org/10.1016/j.compstruct.2022.116096